Environmental Science & Technology

Article

Cite This: Environ. Sci. Technol. 2019, 53, 7887−7892

pubs.acs.org/est

Fate of Mercury in Volatiles and Char during in Situ Gasification Chemical-Looping Combustion of Coal

Jinchen Ma,[†,∥] Daofeng Mei,[‡,∥] Xin Tian,[†] Shibo Zhang,[†] Jianping Yang,[†,§] Chaoquan Wang,[†] Guoping Chen,[†] Yongchun Zhao,*[,†] Chuguang Zheng,[†] and Haibo Zhao*[,†]

[†]State Key Laboratory of Coal Combustion, School of Energy and Power Engineering, Huazhong University of Science and Technology, 1037 Luoyu Road, Wuhan, 430074, PR China

[‡]Key Laboratory of Agricultural Equipment in Mid-lower Yangtze River, Ministry of Agriculture and Rural Affairs, Huazhong Agricultural University, 1 Shizishan Road, Wuhan, 430070, PR China

[§]School of Energy Science and Engineering, Central South University, 932 South Lushan Road, Changsha, 410083, PR China

Supporting Information

ABSTRACT: Mercury emission is an important issue during *in-situ* gasification chemical-looping combustion (*i*G-CLC) of coal. This work focused on experimentally "isolating" two elementary subprocesses (coal pyrolysis and char gasification) during *i*G-CLC of coal, identifying mercury distribution within the two subprocesses, and examining the effects of a hematite oxygen carrier (OC) on the mercury fate. The mercury measurement accuracy was carefully ensured by comparing online measurements (by a VM 3000 instrument) and benchmark measurements (by the standard Ontario Hydro Method, ASTM D6784) as well as repeated tests (10 times for each case). The mercury mass balance was 115% for the entire *i*G-CLC. A total of 44.7% of the mercury was released as the gas phase form within the coal pyrolysis process at a typical CLC operation temperature (950 °C), whereas 13.4% was released during the char gasification process. The release rate and amount of mercury were minimally affected by the presence of OC; however, the OC promoted the conversion of $Hg^0(g)$ to $Hg^{2+}(g)$. Only a small amount of mercury was absorbed by the OC and transported into the air reactor along with carbon residue, released as $Hg^0(g)$ and $Hg^{2+}(g)$ or remained in the OC and coal ash as particulate mercury.

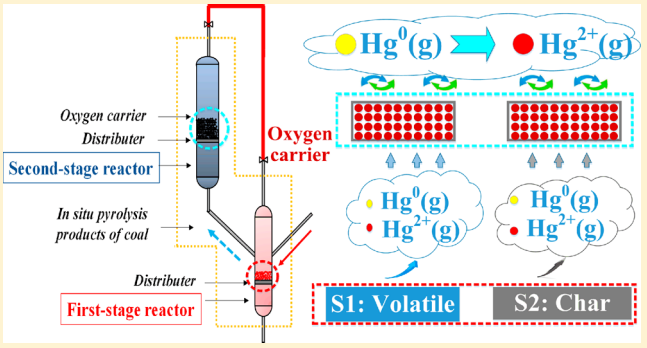

1. INTRODUCTION

Chemical-looping combustion (CLC) has emerged as a promising fossil fuel utilization technology due to the advantages of inherent CO_2 separation.[1] For solid fuel (usually coal) combustion, *in situ* gasification CLC (*i*G-CLC),[2] detailed in the Supporting Information (SI), would be a more feasible mode of CLC.

Mercury, a main pollutant during coal combustion, is detrimental to the environment because of its deleteriousness, bioaccumulation, degradation-resistance and volatility in the ecological system.[3] Generally, mercury is removed by various modified sorbents or catalysts.[4−6] The mercury migration and behaviors in air combustion, gasification and oxy-fuel combustion processes of coal have been extensively investigated.[7−10] However, these behaviors may be very different for *i*G-CLC due to the special factors in the combustion process, that is, the transfer of oxygen in the lattice form and the complexity of the active sites on the OC surface for mercury conversion.[11] Despite this fact, few works focusing on the release and speciation of mercury in *i*G-CLC have been published.[12,13] According to Mendiara et al.,[12,13] mercury was mainly in the form of $Hg^0(g)$ and $Hg^{2+}(g)$ in the fuel reactor (FR) and the air reactor (AR), respectively, according to the tests in a 500W_{th} continuous *i*G-CLC system. Although various operation parameters, including temperature and coal type, were thoroughly investigated in terms of the influence on mercury emissions, more insights into the fate of mercury for *i*G-CLC of coal needs to be well addressed. In the FR of *i*G-CLC, the coal first undergoes coal pyrolysis and char gasification processes, and then the corresponding gaseous products react with the OC, as shown in SI Figure S2. The atmosphere of the FR in *i*G-CLC is similar to that for coal pyrolysis and anaerobic gasification; however, the presence of OC must be considered, especially due to its influence on the formation and transference of different mercury speciation. Moreover, the influence of the OC on the two fundamental processes of *i*G-CLC, that is, coal pyrolysis and char

Received: December 29, 2018
Revised: May 31, 2019
Accepted: June 10, 2019
Published: June 10, 2019

DOI: 10.1021/acs.est.8b06931
Environ. Sci. Technol. 2019, 53, 7887−7892

Table 1. Composition Analyses of XLT Coal and XLT Char

	proximate analysis (wt.%, ad)				ultimate analysis (wt.%, daf)					
	M	V	FC	A	C	H	N	S	O[a]	Hg_{coal}[b]
XLT coal	10.59	49.56	33.40	6.45	45.52	4.20	1.28	0.60	31.36	0.565
XLT char	3.64	6.45	77.79	12.12	78.60	0.60	1.17	0.68	3.19	0.060

[a]By difference. [b]With units of $\mu g/g$.

gasification, is unclear. Insights into this influence are important for understanding the mercury release characteristics and speciation mechanism and thus developing the strategy/technology for mercury control.

The objective of this work was to study the fate of mercury in coal pyrolysis and char gasification under the *i*G-CLC mode for coal combustion. Specifically, a two-stage fluidized bed reactor in bench scale was adopted to simulate the CLC pattern. In the first-stage reactor, raw coal was pyrolyzed to generate the in situ volatiles that were directly introduced into the second-stage reactor. Tests using hematite OC or silica sand as bed material were conducted to study the fate of mercury in volatiles. To investigate the fate of mercury in char and coal, a bench-scale batch fluidized bed reactor was used under the *i*G-CLC condition in which the as-prepared char/raw coal was reacted with the hematite OC particles. The contents of $Hg^0(g)$ and $Hg^{2+}(g)$ in flue gas and the particulate mercury Hg(p) in ash and/or the OC were measured to explore the fate and distribution of mercury during *i*G-CLC.

2. MATERIALS AND METHODS

2.1. Materials. The same hematite as that tested previously in a 5 kW_{th} interconnected fluidized bed reactor[14] was used as the OC in this work. The OC was calcined at 900 °C and then sieved to a range of 125−300 μm, making it ready for tests. The fresh calcined hematite OC particles mainly contained 65.9 wt % Fe_2O_3, 25.2 wt % SiO_2, 5.4 wt % Al_2O_3, and no any mercury was detected, as seen in SI Table S1.

A high-mercury lignite from Xiaolongtan (abbreviated as XLT), China, was sieved to a diameter of 120−200 μm and used as a solid fuel. Meanwhile, the corresponding XLT char was produced by devolatilizing the coal in a tube furnace at 950 °C for 30 min in a high purity N_2 atmosphere. The proximate and ultimate analyses of XLT coal and XLT char, as well as their mercury content (Hg_{coal}, determined by a Lumex RA-915M), are listed in Table 1. This XLT lignite can be classified as a high-mercury coal due to the high concentration of Hg contained.[15,16] Moreover, the ash of XLT coal was also analyzed to obtain the chemical composition, as shown in SI Table S2, where no mercury was detected.

2.2. Experimental Setup. Two types of bench-scale reactors were applied for the tests, that is, a two-stage fluidized bed reactor (TFR) and a batch fluidized bed reactor (BFR), as shown in Figure 1a and b, respectively. The TFR is consisted of a lower first-stage reactor for coal pyrolysis and a higher second-stage reactor loading the OC or silica sand as bed material. In this sense, coal and the bed material were separately located; thus, the influence of the OC on the mercury content in volatiles can be separately studied without the effect of char, and vice versa. For each test in the bench-scale TFR, 0.52 g XLT coal was fed to the first-stage reactor, and 60 g OC or silica sand (referred to as the blank test) was loaded in the second-stage reactor. The in situ volatiles produced from the first-stage reactor were directed to the

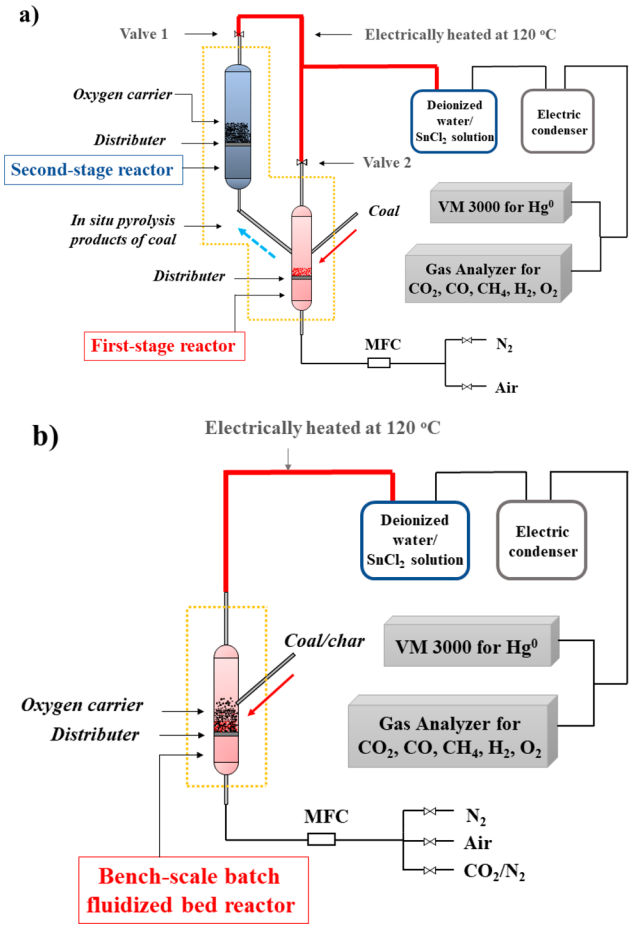

Figure 1. A schematic view of the experimental setup: (a) bench-scale two-stage fluidized bed reactor and (b) bench-scale batch fluidized bed reactor.

second-stage reactor to react with the OC or to contact with silica sand without a cooling-down process. In the case of the bench-scale BFR, solid fuels were directly contacted with the OC or silica sand because they were all located at the same reactor, as shown in Figure 1b. For the test with XLT char, 60 g OC or silica sand (as the blank test) was used as bed material to identify the effect of the OC on the mercury speciation during the char gasification. In each test with char, 0.22 g XLT char, equivalent to that in 0.52 g XLT coal, was used as fuel in the BFR. The same procedure was repeated in the BFR using 0.52 g XLT coal to simulate the typical *i*G-CLC of coal. All tests were conducted at a CLC-representative temperature of 950 °C. For the gasification of coal and char, CO_2 instead of H_2O was used as a gasifying agent to avoid the influence of H_2O on mercury speciation.[17,18] Details of the experimental conditions and procedures are included in SI Section S2.2. The outlet gas stream of the TFR and BFR was pretreated and sent to the online analyzers to determine the concentrations of typical gases (CO_2, CO, CH_4, H_2, and O_2) and elemental

DOI: 10.1021/acs.est.8b06931
Environ. Sci. Technol. 2019, 53, 7887−7892

Table 2. CO_2, CO, and CH_4 Yields and Carbon Conversion (X_C) during Reduction for the Ten-Times Repeated Tests

tests	CO_2 yield (%)	CO yield (%)	CH_4 yield (%)	X_C (−)
2	93.13 ± 0.54	4.12 ± 0.60	3.11 ± 0.50	0.52 ± 0.026
4	93.00 ± 0.62	6.70 ± 0.38	0	0.94 ± 0.028 for char
5	91.33 ± 1.13	6.53 ± 0.53	3.80 ± 0.94	0.94 ± 0.025

mercury $Hg^0(g)$. Solid samples were collected and then subjected to offline analyzers to determine the mercury contents.

2.3. Mercury Measurement. The real concentration of $Hg^0(g)$ in the exhaust gas stream was determined using online cold vapor atomic absorption spectroscopy (VM 3000 Mercury Vapor Monitor, Mercury Instruments, Germany) after normalization with deionized water and condensation with an electrical cooler. However, the real concentration of $Hg^{2+}(g)$ cannot be directly attained with the same analyzer. Therefore, a $SnCl_2$ solution was used to first reduce all the $Hg^{2+}(g)$ to $Hg^0(g)$, so that the $Hg^0(g)$ detected by the VM 3000 was the total concentration of gaseous mercury, which was denoted as $Hg^T(g)$. In this sense, the concentration of $Hg^{2+}(g)$ can be calculated as the difference between $Hg^T(g)$ and $Hg^0(g)$. The mercury contents in coal ash and OC particles, Hg(p), were measured by an offline analyzer (Lumex RA-915 M with PYRO−915+ pyrolysis equipment (Ohio Lumex Company, Russia)) after cooling down of the reactors. The distribution of mercury in various forms was also determined according to the standard Ontario Hydro Method (OHM),[19] as shown in SI Figure S4. Mercury in all OHM digestion solutions was detected by a double channel atomic fluorescence spectrometry mercury analyzer (AFS930).

Due to the small amount of mercury, the accuracy of mercury measurements was of primary importance and of particular concern for this work. First, analyzers with high accuracy (0.1 $\mu g/Nm^3$ for VM 3000, 0.1 ng/g for Lumex RA-915 M and 0.001 $\mu g/L$ for AFS930) were used for mercury measurements. Second, the influence of H_2O and SO_2 on the accuracy of the VM3000 was minimized by (i) using CO_2 as gasifying agent in reactors since the effect of H_2O on the accuracy of the VM 3000 is more significant; (ii) ensuring that the H_2O in the product gas was electrically condensed before sending it to the analyzer due to its influence on mercury speciation;[17,18] and (iii) calibrating the concentration of $Hg^0(g)$ under relevant concentrations of SO_2 and CO_2 for pyrolysis and char gasification. Third, the results of the online measurements (by the VM 3000) were compared with the offline mercury measurements based on the OHM, as shown in SI Section S4, where good consistency between the two methods was observed. Finally, each case was repeated 10 times (see SI Section S4) to increase the confidence of the reliability of the experimental data.

2.4. Data Evaluation. The amount of gaseous mercury (V_{Hg^i}) with units of μg was calculated as

$$V_{Hg^i} = \int_0^{t_{total}} F_j \cdot y_{Hg^i} dt \quad (1)$$

Here, F_j represents the volumetric flow rate of the flue gas during the different stages in the experiments, which is calculated on the basis of the nitrogen balance;[20] j represents the reduction stage or oxidation stage; y_{Hg^i} is the mercury concentration ($\mu g/m^3$) in the flue gases, i represents the gaseous mercury species ($Hg^0(g)$ or $Hg^{2+}(g)$); and t_{total} is the duration time of stage j.

The release fraction of gaseous mercury (ω_{Hg^i}) was calculated as the mass ratio of detectable gaseous mercury i to the total mercury in coal ($m_{Hg_{coal}}$):

$$\omega_{Hg^i} = \int_0^t F_j \cdot Hg^i dt / m_{Hg_{coal}} \times 100\% \quad (2)$$

The CLC performance indexes were calculated according to the methods introduced in our previous research,[20] which are also shown in SI Section S3.

3. RESULTS AND DISCUSSION

3.1. CLC Performance. The CLC experiment of in situ volatiles (test 2, in the bench-scale two-stage fluidized bed reactor) using hematite as the OC was first conducted at 950 °C. As shown in Table 2, the hematite had a high reactivity toward volatiles, with an average CO_2 yield of 93.13 ± 0.51% in test 2 (see SI Table S3) using the TFR. For the *i*G-CLC of the as-prepared char (test 4, see SI Table S3), the CO_2 yield was 93.00 ± 0.59% in average, which was attributed to a high oxygen-to-fuel ratio (~4.0 according to the ultimate analysis of XLT char). Thus, a low CO yield of 6.70 ± 0.36% was attained in average. In the *i*G-CLC of raw coal (test 5 in the BFR, see SI Table S3), the average CO_2 yield was decreased to 91.33 ± 1.07%, whereas a higher total yield of CO and CH_4 than that for test 2 was seen in Table 2. This result was ascribed to the low oxygen-to-fuel ratio (~2.0 according to the ultimate analysis of XLT coal). It is also worth noting that the average carbon conversion in the *i*G-CLC experiments was high, that is, 0.94 ± 0.027 for test 4 and 0.94 ± 0.024 for test 5. This behavior suggests that the carbon residue is quite low.

3.2. Fate of Mercury in Volatiles. The pyrolysis process was accomplished in 90 s for this type of lignite, which was indicated by the reduction of carbonaceous gases to zero in the blank test, as shown in the upper right-hand corner of Figure 2. After the pyrolysis process, 180 s was set as the purge process

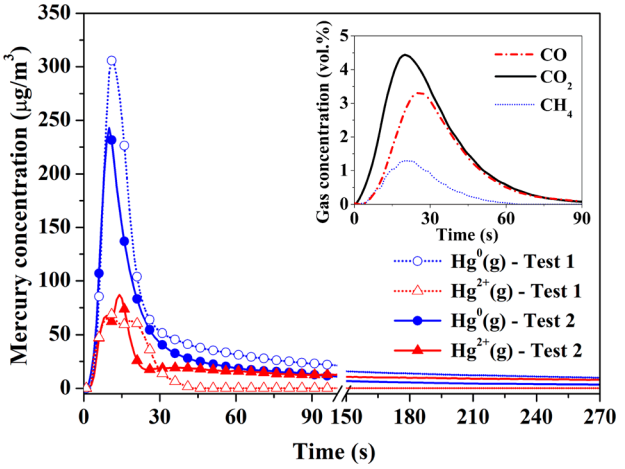

Figure 2. $Hg^0(g)$ and $Hg^{2+}(g)$ concentrations during the coal pyrolysis process for the blank experiment (test 1) and the CLC experiment (test 2).

DOI: 10.1021/acs.est.8b06931
Environ. Sci. Technol. 2019, 53, 7887−7892

time using N_2 as the inert gas. As expected, the mercury with high volatility was rapidly released in the gas phase with volatiles during these two processes, as shown in Figure 2. Two peaks of the $Hg^{2+}(g)$ concentration were observed during the XLT coal pyrolysis process (test 1 with silica sand as bed material, see SI Table S3). This result was explained by different release rates of different existing forms of mercury.[21] $Hg^0(g)$ was the main species for coal pyrolysis because of the reducing atmosphere, which is consistent with previous research.[22]

When the OC was present in the CLC reactor (test 2, see SI Table S3), the peak value of the $Hg^0(g)$ concentration decreased, while the $Hg^{2+}(g)$ concentration increased, as shown in Figure 2. Furthermore, the concentration of $Hg^{2+}(g)$ was maintained at a relatively stable value of 20 $\mu g/Nm^3$ from 50 s and gradually exceeded the concentration of $Hg^0(g)$ at the later stage (>60 s). This result indicated that the oxidization of $Hg^0(g)$ to $Hg^{2+}(g)$ was enhanced, probably because of the presence of the OC. The possible functions of the OC for the oxidation of $Hg^0(g)$ are discussed in Sections 3.3 and 3.4 of this work.

3.3. Fate of Mercury in Char. The $Hg^0(g)$, $Hg^{2+}(g)$, and $Hg^T(g)$ release fractions as a function of time are shown in Figure 3. Accordingly, the following four findings can be

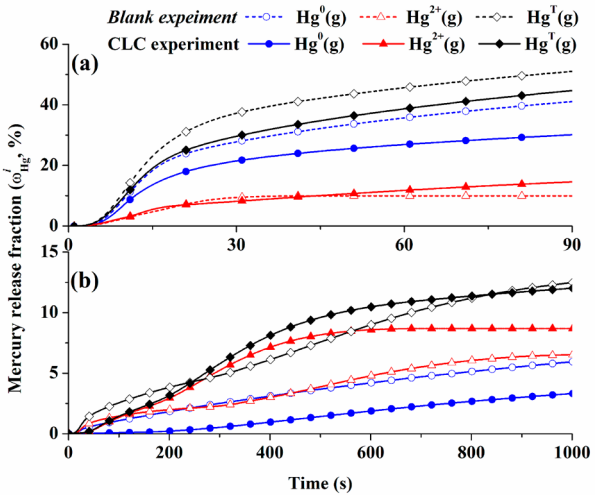

Figure 3. $Hg^0(g)$, $Hg^{2+}(g)$, and $Hg^T(g)$ release fractions within the separate (a) coal pyrolysis process and (b) char gasification process.

drawn: (i) During the coal pyrolysis or char gasification process, the total gaseous mercury release fraction versus time showed a similar trend in both the CLC experiment and the blank experiment, which indicated that the mercury release rate and amount were minimally affected by the presence of the OC. The small difference was attributed to the physisorption of mercury on the OC according to the density functional theory (DFT) simulations.[23,24] (ii) At the same time point, the released fraction of $Hg^0(g)$ in the blank experiment was always higher than that in the CLC experiment, whereas the $Hg^{2+}(g)$ fraction displayed an obviously opposite trend, which was ascribed to the presence of OC, promoting the oxidization of $Hg^0(g)$ to $Hg^{2+}(g)$. (iii) approximately half of the mercury in coal was released in the 90 s pyrolysis process (approximately 51.0% for the blank experiment and 44.7% for the CLC experiment based on the total mercury in coal), which is certainly ascribed to the high volatility of mercury at a high operation temperature (950 °C). After the pyrolysis process, the gaseous mercury was continuously released during the N_2 purging process, accounting for approximately 19.6% of the total mercury in coal. This trend can be explained by the fact that various forms of mercury could be released at 950 °C, as suggested by Luo et al.[21] (iv) The release rates of $Hg^0(g)$ and $Hg^{2+}(g)$ during the process of char gasification were much lower than those during the process of coal pyrolysis, mainly because of the relatively slow gasification of char in a CO_2 atmosphere.

As mentioned above, the presence of the OC prompted the conversion of $Hg^0(g)$ to $Hg^{2+}(g)$ because of the following factors. (i) The high oxygen-to-fuel ratio provides more lattice oxygen for the oxidation of mercury from $Hg^0(g)$ to $Hg^{2+}(g)$. (ii) The flue gas components were changed after the volatile matter or gasification products were converted by the OC, which influenced the mercury distribution. As reported,[25] H_2S and CO could inhibit the oxidization of mercury at 750 °C.[26] In CLC, these inhibiting compounds were efficiently converted by the OC,[27] such as H_2S to SO_2 and CO to CO_2 (see more details in SI Section S4.2). Therefore, the inhibitory effects of gas compounds on the oxidation of $Hg^0(g)$ to $Hg^{2+}(g)$ were weakened. (iii) The oxidation of $Hg^0(g)$ to $Hg^{2+}(g)$ by HCl (usually present in flue gas) can be enhanced due to the more active sites on the OC surface via the Eley−Rideal[28] and/or heterogeneous oxidation mechanisms.[29]

3.4. Mercury Distribution. Furthermore, the gaseous mercury released within the oxidization stage of the OC and/or carbon residue used in the CLC and blank experiments was measured. The particulate mercury in coal ash and/or the OC was also determined. In the CLC test of in situ volatiles (test 2 in SI Table S3), coal was introduced into the first pyrolysis reactor, and the OC was loaded in the second CLC reactor. Therefore, the particulate mercury in the OC or ash can be distinguished. The results showed that there was no mercury detected in the sole ash, as shown in SI Table S2. In the *i*G-CLC experiments of char (test 3 in SI Table S3) and coal (test5 in SI Table S3), the particulate mercury in the mixture of coal ash and the OC was measured due to the difficulty in completely separating the OC and coal ash.

The released amounts of all mercury species are summarized in Figure 4. According to the measurement results in the CLC of in situ volatiles, most of the mercury in coal (approximately 44.7% based on the total mercury in coal) was released in the process of coal pyrolysis (0−90 s in test 1) as gas phase (30.1% $Hg^0(g)$ and 14.6% $Hg^{2+}(g)$ based on the total mercury in the coal). The amount of gaseous mercury in *i*G-CLC of the as-prepared char was quite small, that is, 4.6% $Hg^0(g)$ and 8.8% $Hg^{2+}(g)$ based on the total mercury in the coal. Compared to the measured gaseous mercury in the fuel reactor, the amount of gaseous mercury detected during the oxidation stage was smaller, with values of 1.5∼5.6% (all based on the total mercury in coal). There was less particulate mercury remaining in the OC and/or ash (1.0−1.8% based on the total mercury in coal). A small amount of gaseous mercury was released within the oxidization stage of the OC in the CLC experiment of in situ volatiles, as shown in SI Figure S9. These results could be attributed to the porous structure and large surface area of the OC as well as the produced Fe_3O_4 surface with reactive oxygen sites, which were responsible for the physical adsorption and/or oxidization of the mercury.[23,30]

In the *i*G-CLC experiment of raw XLT coal, the fractions of $Hg^0(g)$ and $Hg^{2+}(g)$ were 55% and 43%, respectively, during

DOI: 10.1021/acs.est.8b06931
Environ. Sci. Technol. 2019, 53, 7887−7892

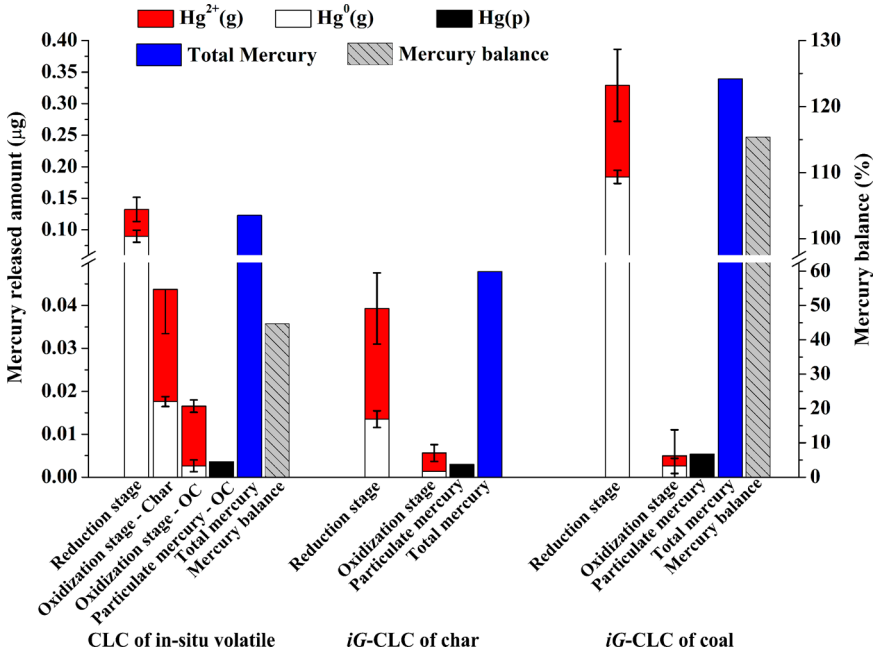

Figure 4. Mercury released amount and distribution.

the reduction process, whereas they were 0.6% and 0.9%, respectively, during the oxidization stage. This result is in line with those reported by Mendiara et al.[12,13] where $Hg^0(g)$ and $Hg^{2+}(g)$ were the main states of mercury in the reduction and oxidization stages, respectively. However, the concentration values of each mercury species were quite different from those of Mendiara et al.,[12] mainly because of the different reactors used. In the case of Mendiara et al.,[12] a $500W_{th}$ continuous CLC reactor was used, whereas discontinuous fluidized bed reactors were involved in this work; thus, different residence times of coal in the reactors can be inferred. The char gasification process required approximately 1000 s, which could result in more char being entrained into the AR of the $500W_{th}$ system used by Mendiara et al.[12] However, in our case, the residence time of coal can be as long as 1400 s due to the use of a discontinuous reactor. Thus, the fraction of released mercury in pyrolysis was approximately 44.7% in the first 90 s of volatilization, which continually increased to approximately 92.2% after 1400 s (with an extended N_2 purge process in test 1). Thus, the different configurations of reactors in the study by Mendiara et al.[12] and in our present study can explain the different fractions of released mercury in each reactor.

The mercury balance was calculated based on the total mercury in coal (Hg_{coal}), which is also presented in Figure 4. The mercury balance was 115% in the whole *i*G-CLC process (test 5, see SI Table S3), which is within an acceptable range (70∼130%).

In summary, the hematite OC had almost no effect on the total fraction of gaseous mercury ($Hg^T(g)$) released. However, an OC with sufficient active lattice oxygen could promote the conversion of $Hg^0(g)$ to $Hg^{2+}(g)$. This phenomenon was also partially because some gaseous components, for example, H_2S and CO, which inhibited the $Hg^0(g)$ oxidization, were converted by the lattice oxygen of the OC particles. Meanwhile, the generated Fe_3O_4 and porous structure of the OC during redox cycles were beneficial for mercury absorption and conversion. Most of the mercury in coal was released during the CLC of in situ volatiles due to the high volatility of mercury. Besides, the amount of gaseous mercury released in the oxidization stage of the OC and carbon residue (for an air reactor) and the amount of particulate mercury in the OC and/or coal ash were extremely low.

■ ASSOCIATED CONTENT

Supporting Information

The Supporting Information is available free of charge on the ACS Publications website at DOI: 10.1021/acs.est.8b06931.

Schematics of CLC and *i*G-CLC (Figure S1 and S2); Details of the bench-scale two-stage fluidized bed reactor and the batch fluidized bed reactor (Figure S3); Ontario Hydro Method (Figure S4); $Hg^0(g)$ concentration at five repeated cycles for tests 2 and 5 (Figure S5); Sulfurous gases distribution and the CO, CH_4, and CO_2 distribution during the pyrolysis process at blank experiment and *i*G-CLC experiment (Figure S6); Carbon conversion during the *i*G-CLC of volatile at tests 1 and 2 (Figure S7); Mercury released amount and balance at blank experiments (Figure S8); $Hg^0(g)$ and $Hg^{2+}(g)$ concentration at *i*G-CLC process and $Hg^0(g)$, $Hg^{2+}(g)$ and $Hg^T(g)$ release fraction during the *i*G-CLC process (Figure S9). Tables S1 and S2, Chemical compositions of the hematite and XLT coal ash; Table S3, Operation conditions in this work; Table S4, Gaseous mercury distribution; Table S5, CO_2, CO, and CH_4 Yields and Carbon Conversion (X_C) in the reduction process, with the relative standard deviation (RSD) included in brackets for the 10-times repeated tests (PDF)

■ AUTHOR INFORMATION

Corresponding Authors

*(Y.Z.) Phone: 86−27−87542417; fax: 86−27−87545526; e-mail: yczhao@hust.edu.cn.
*(H.Z.) Phone: 86−27−87542417; fax: 86−27−87545526; e-mail: hzhao@mail.hust.edu.cn.

DOI: 10.1021/acs.est.8b06931
Environ. Sci. Technol. 2019, 53, 7887−7892

ORCID

Yongchun Zhao: 0000-0001-7463-7950
Haibo Zhao: 0000-0002-2693-4499

Author Contributions

‖J.M. and D.M. contributed equally on experiment operation and manuscript preparation. H.Z. conceived the research, designed the experiment and guided the data analysis.

Notes

The authors declare no competing financial interest.

■ ACKNOWLEDGMENTS

This work was founded by "National Key R&D Program of China (2016YFB0600801)", "National Natural Science Foundation of China (51606077 and 51522603)", "Fundamental Research Funds for the Central Universities (2662016QD043)", and "Hubei Provincial Natural Science Foundation of China (2018CFB376)". Meanwhile, the staff from the Analytical and Testing Center, Huazhong University of Science and Technology, are appreciated for the relevant analytical work.

■ REFERENCES

(1) Ishida, M.; Jin, H. A novel combustor based on chemical-looping reactions and its reaction kinetics. *J. Chem. Eng. Jpn.* **1994**, *27* (3), 296−301.

(2) Dennis, J. S.; Scott, S. A.; Hayhurst, A. N. *In situ* gasification of coal using steam with chemical looping: a technique for isolating CO_2 from burning a solid fuel. *J. Energy Inst.* **2006**, *79* (3), 187−190.

(3) Gharebaghi, M.; Hughes, K. J.; Porter, R. T. J.; Pourkashanian, M.; Williams, A. Mercury speciation in air-coal and oxy-coal combustion: a modelling approach. *Proc. Combust. Inst.* **2011**, *33* (2), 1779−1786.

(4) Chen, W.; Pei, Y.; Huang, W.; Qu, Z.; Hu, X.; Yan, N. Novel effective catalyst for elemental mercury removal from coal-fired flue gas and the mechanism investigation. *Environ. Sci. Technol.* **2016**, *50* (5), 2564−2572.

(5) Zhang, B.; Zeng, X.; Xu, P.; Chen, J.; Xu, Y.; Luo, G.; Xu, M.; Yao, H. Using the novel method of nonthermal plasma to add Cl active sites on activated carbon for removal of mercury from flue gas. *Environ. Sci. Technol.* **2016**, *50* (21), 11837−11843.

(6) Yang, J.; Zhao, Y.; Chang, L.; Zhang, J.; Zheng, C. Mercury adsorption and oxidation over cobalt oxide loaded magnetospheres catalyst from fly ash in oxyfuel combustion flue gas. *Environ. Sci. Technol.* **2015**, *49* (13), 8210−8218.

(7) Selin, H.; VanDeveer, S. D. Mapping institutional linkages in European air pollution politics. *Global Environmental Politics* **2003**, *3* (3), 14−46.

(8) Galbreath, K. C.; Zygarlicke, C. J. Mercury speciation in coal combustion and gasification flue gases. *Environ. Sci. Technol.* **1996**, *30* (8), 2421−2426.

(9) Yang, J.; Ma, S.; Zhao, Y.; Zhang, J.; Liu, Z.; Zhang, S.; Zhang, Y.; Liu, Y.; Feng, Y.; Xu, K.; Xiang, J.; Zheng, C. Mercury emission and speciation in fly ash from a 35 MW_{th} large pilot boiler of oxyfuel combustion with different flue gas recycle. *Fuel* **2017**, *195*, 174−181.

(10) Fernandez-Miranda, N.; Lopez-Anton, M. A.; Torre-Santos, T.; Diaz-Somoano, M.; Martinez-Tarazona, M. R. Impact of oxy-fuel conditions on elemental mercury re-emission in wet flue gas desulfurization systems. *Environ. Sci. Technol.* **2016**, *50* (13), 7247−7253.

(11) Li, J.-H.; Lin, C.-F.; Qin, W.; Xiao, X.-B.; Wei, L. Synergetic effect of mercury adsorption on the catalytic decomposition of CO over perfect and reduced Fe_2O_3 [001] surface. *Acta Physico-Chimica Sinica* **2016**, *32* (11), 2717−2723.

(12) Mendiara, T.; Izquierdo, M. T.; Abad, A.; Gayán, P.; García-Labiano, F.; de Diego, L. F.; Adánez, J. Mercury release and speciation in chemical looping combustion of coal. *Energy Fuels* **2014**, *28* (4), 2786−2794.

(13) Mendiara, T.; Izquierdo, M. T.; Abad, A.; de Diego, L. F.; García-Labiano, F.; Gayán, P.; Adánez, J. Release of pollutant components in CLC of lignite. *Int. J. Greenhouse Gas Control* **2014**, *22*, 15−24.

(14) Ma, J.; Zhao, H.; Tian, X.; Wei, Y.; Zhang, Y.; Zheng, C. Continuous operation of interconnected fluidized bed reactor for chemical looping combustion of CH_4 using hematite as oxygen carrier. *Energy Fuels* **2015**, *29* (5), 3257−3267.

(15) Dai, S.; Zeng, R.; Sun, Y. Enrichment of arsenic, antimony, mercury, and thallium in a Late Permian anthracite from Xingren, Guizhou, Southwest China. *Int. J. Coal Geol.* **2006**, *66* (3), 217−226.

(16) Dai, S.; Ren, D.; Chou, C.-L.; Finkelman, R. B.; Seredin, V. V.; Zhou, Y. Geochemistry of trace elements in Chinese coals: A review of abundances, genetic types, impacts on human health, and industrial utilization. *Int. J. Coal Geol.* **2012**, *94* (1), 3−21.

(17) Sekine, Y.; Sakajiri, K.; Kikuchi, E.; Matsukata, M. Release behavior of trace elements from coal during high-temperature processing. *Powder Technol.* **2008**, *180* (1), 210−215.

(18) Helble, J. J.; Mojtahedi, W.; Lyyränen, J.; Jokiniemi, J.; Kauppinen, E. Trace element partitioning during coal gasification. *Fuel* **1996**, *75* (8), 931−939.

(19) ASTM D 6784−02. *Standard Test Method for Elemental, Oxidized, Particle-Bound and Total Mercury in Flue Gas Generated from Coal-Fired Stationary Sources (Ontario Hydro Method)*; ASTM: West Conshohocken, PA, 2002.

(20) Ma, J.; Tian, X.; Zhao, H.; Bhattacharya, S.; Rajendran, S.; Zheng, C. Investigation of two hematites as oxygen carrier and two low-rank coals as fuel in chemical looping combustion. *Energy Fuels* **2017**, *31* (2), 1896−1903.

(21) Luo, G.; Yao, H.; Xu, M.; Gupta, R.; Xu, Z. Identifying modes of occurrence of mercury in coal by temperature programmed pyrolysis. *Proc. Combust. Inst.* **2011**, *33* (2), 2763−2769.

(22) Li, Y.; Zhang, J.; Zhao, Y.; Zheng, C. Volatility and speciation of mercury during pyrolysis and gasification of five Chinese coals. *Energy Fuels* **2011**, *25* (9), 3988−3996.

(23) Guo, P.; Guo, X.; Zheng, C.-G. Computational insights into interactions between Hg species and α-Fe_2O_3 (0 0 1). *Fuel* **2011**, *90* (5), 1840−1846.

(24) Zhang, J.; Qin, W.; Dong, C.; Yang, Y. Density functional theory study of elemental mercury adsorption on Fe_2O_3[104] and its effect on carbon deposit during chemical looping combustion. *Energy Fuels* **2016**, *30* (4), 3413−3418.

(25) Yang, J.; Zhao, Y.; Zhang, S.; Liu, H.; Chang, L.; Ma, S.; Zhang, J.; Zheng, C. Mercury removal from flue gas by magnetospheres present in fly ash: role of iron species and modification by HF. *Fuel Process. Technol.* **2017**, *167*, 263−270.

(26) Lu, D. Y.; Granatstein, D. L.; Rose, D. J. Study of mercury speciation from simulated coal gasification. *Ind. Eng. Chem. Res.* **2004**, *43* (17), 5400−5404.

(27) Ma, J.; Wang, C.; Zhao, H.; Xin, T. Sulfur fate during the lignite pyrolysis process in a chemical looping combustion environment. *Energy Fuels* **2018**, *32* (4), 4493−4501.

(28) Tao, L.; Guo, X.; Zheng, C. Density functional study of Hg adsorption mechanisms on α-Fe_2O_3 with H_2S. *Proc. Combust. Inst.* **2013**, *34* (2), 2803−2810.

(29) Yang, Y.; Liu, J.; Shen, F.; Zhao, L.; Wang, Z.; Long, Y. Kinetic study of heterogeneous mercury oxidation by HCl on fly ash surface in coal-fired flue gas. *Combust. Flame* **2016**, *168*, 1−9.

(30) Xue, L.; Liu, T.; Guo, X.; Zheng, C. Hg oxidation reaction mechanism on Fe_2O_3 with H_2S: comparison between theory and experiments. *Proc. Combust. Inst.* **2015**, *35* (3), 2867−2874.

DOI: 10.1021/acs.est.8b06931
Environ. Sci. Technol. 2019, 53, 7887−7892